

Cite this: DOI: 10.1039/c1cp22692d

www.rsc.org/pccp

PAPER

# A large sample volume magic angle spinning nuclear magnetic resonance probe for *in situ* investigations with constant flow of reactants

Jian Zhi Hu,\* Jesse A. Sears, Hardeep S. Mehta, Joseph J. Ford, Ja Hun Kwak, Kake Zhu, Yong Wang, Jun Liu, David W. Hoyt and Charles H. F. Peden\*

Received 22nd August 2011, Accepted 4th October 2011

DOI: 10.1039/c1cp22692d

A large-sample-volume constant-flow magic angle sample spinning (CF-MAS) NMR probe is reported for *in situ* studies of the reaction dynamics, stable intermediates/transition states, and mechanisms of catalytic reactions. In our approach, the reactants are introduced into the catalyst bed using a fixed tube at one end of the MAS rotor while a second fixed tube, linked to a vacuum pump, is attached at the other end of the rotor. The pressure difference between both ends of the catalyst bed inside the sample cell space forces the reactants flowing through the catalyst bed, which improves the diffusion of the reactants and products. This design allows the use of a large sample volume for enhanced sensitivity and thus permitting *in situ*  $^{13}\text{C}$  CF-MAS studies at natural abundance. As an example of application, we show that reactants, products and reaction transition states associated with the 2-butanol dehydration reaction over a mesoporous silicalite supported heteropoly acid catalyst (HPA/meso-silicalite-1) can all be detected in a single  $^{13}\text{C}$  CF-MAS NMR spectrum at natural abundance. Coke products can also be detected at natural  $^{13}\text{C}$  abundance and under the stopped flow condition. Furthermore,  $^1\text{H}$  CF-MAS NMR is used to identify the surface functional groups of HPA/meso-silicalite-1 under the condition of *in situ* drying. We also show that the reaction dynamics of 2-butanol dehydration using HPA/meso-silicalite-1 as a catalyst can be explored using  $^1\text{H}$  CF-MAS NMR.

## 1. Introduction

A detailed understanding of mechanisms involved in a catalytic reaction requires that we identify the nature of active sites and reaction intermediates, and that we probe dynamic processes starting when reactants enter the reaction zone until the final products are eluted from the system.<sup>1</sup> For reactions involving simple species, *in situ* techniques such as UV-visible and IR spectroscopies are typically used to probe the nature of adsorbed intermediates.<sup>2</sup> For many important reactions such as selective oxidation of organics, reaction products and intermediates are far more complex and are difficult to identify using a single spectroscopic tool.<sup>2</sup> High resolution magic angle spinning (MAS) nuclear magnetic resonance (NMR) spectroscopy is one of the most powerful and versatile techniques for studying molecular structure and dynamics regardless of whether the system is a solid, semi-solid, or a heterogeneous system containing a mixture of *e.g.*, solid, semi-solid, liquid, and gaseous phases. This makes MAS NMR an attractive tool for *in situ* investigations of reaction dynamics and intermediates,

as well as the properties of active sites in a heterogeneous catalytic reaction.

A number of *in situ* MAS NMR techniques have been developed<sup>3–23</sup> and their significance in the field of heterogeneous catalysts has been reviewed recently.<sup>5,11</sup> Among them, the method of constant flow magic angle spinning (CF-MAS) NMR, introduced by Hunger and Horvath,<sup>6</sup> closely simulates realistic catalytic reaction conditions in cases where pressure control is not required; *i.e.*, reactions are carried out under ambient pressure conditions. In Hunger's design, a constant flow of the reactants into the reactor (*i.e.*, the MAS rotor) is realized by injecting a carrier gas (*e.g.*, nitrogen) containing vapors of reactants *via* an injection tube. The injection tube, made of glass or ceramics, is static and is inserted into the sample volume of a MAS NMR rotor *via* an axially placed hole in the rotor cap. The catalyst is shaped to a hollow cylinder that rotates with the rotor. The reactants are injected into the inner space of the cylindrical catalyst bed and flow from the bottom to the top of the sample volume inside the MAS NMR rotor reactor. The product stream plus un-reacted reactants leave the sample volume *via* an annular gap in the rotor cap at the same end where the reactants flow in. This design works remarkably well if the thickness of the catalyst bed is thin, where penetration of the reactants into and the elution of the products out of the catalyst bed are effective.

Institute for Integrated Catalysis, and Environmental Molecular Sciences Laboratory, Pacific Northwest National Laboratory Richland, Washington 99354, USA. E-mail: Jianzhi.Hu@pnl.gov, Chuck.Peden@pnl.gov; Fax: (509) 371-6546; Tel: (509) 371-6544(509) 371-6501

Thus, this design can only use a small amount of catalyst sample even with large sample volume rotors, thus limiting the sensitivity of *in situ* constant flow MAS NMR. In order for an *in situ*  $^{13}\text{C}$  MAS NMR spectrum to be acquired in a reasonable amount of time,  $^{13}\text{C}$  isotope enriched reactants are required for sensitivity enhancement. Considering that for many catalyst reaction systems isotope enriched compounds are either very expensive or simply unavailable commercially, it is thus important to develop a CF-MAS probe that enables *in situ* NMR studies using reactants that contain carbon at natural abundance. One way to increase the signal-to-noise (S/N) ratio in such studies is to use more samples since S/N is approximately proportional to the sample volume.<sup>24</sup>

To our knowledge, *in situ* constant flow MAS of Hunger and coworker's design, with MAS rotor larger than 7.5 mm, has not yet been explored. This is largely due to concerns that S/N will be inadequate since reactions only take place in the shallow portion of catalyst bed even if a thickened catalyst bed is used in the same design as Hunger's. In this work, we report a 9.5 mm outside diameter large-sample-volume CF-MAS probe for sensitivity enhancement so that *in situ*  $^{13}\text{C}$  CF-MAS NMR at natural abundance can be achieved. In our approach, the reactants in a carrier gas, such as nitrogen, flow into the catalyst bed using a fixed tube at one end of the rotor while a second fixed tube, linked to a vacuum pump, is attached at the other end of the MAS rotor to facilitate a flow through the catalyst bed by the pressure difference at both ends of the sample. The flow through catalyst bed improves the diffusion of the reactants and products, allowing the use of a large sample volume and thus permitting *in situ*  $^{13}\text{C}$  CF-MAS NMR studies at natural abundance. The aim of this paper is to describe the features of the current design of this *in situ* NMR spectroscopy reactor, and to provide some brief initial examples of its capabilities to perform catalysis science.

## 2. Methods

Fig. 1 shows the essential components of our large sample volume *in situ* CF-MAS probe, consisting of a 9.5 mm MAS rotor (Fig. 1a and b) and a MAS probe (Fig. 1c). The MAS rotor, *i.e.*, the reactor, when fully assembled (Fig. 1a), resembles a commercial MAS rotor. The rotor sleeve, labeled as "1" is a commercially available zirconium MAS rotor with outside diameter (OD) of 9.5 mm, inner diameter (ID) of 8.5 mm and height of 40 mm. The rotor tip, "2", is a modified commercial Kel-F or Vespel pencil type spin tip, where a center through hole is drilled to allow for the insertion of a static tube, "10" attached to a vacuum pump, into the inner space of the MAS rotor as illustrated in Fig. 1b and c. The internal structures of the MAS rotor are detailed in Fig. 1c, where parts "6" and "7" are end plugs made of ceramics such as Macor, "4" and "5" are layers of glass wool with layer thickness of approximately 1 mm. The combined use of the end plugs and the glass wool is to keep the catalyst in the sample cell space "3". A center thread hole was drilled inside the end plug "6" for guiding the injection tube "8" into the MAS rotor. The thread is used for the convenience of plug removal using a screw tool. This center thread hole is linked to seven holes, consisting of a straight hole at the center and six tilted holes evenly distributed around the

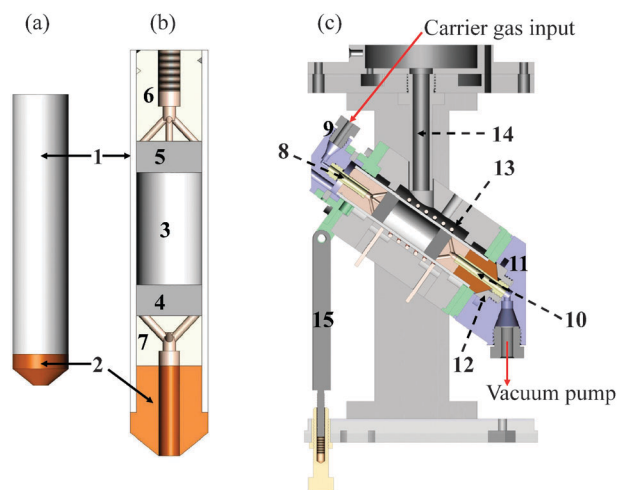


**Fig. 1** Schematic of the large sample volume CF-MAS probe. (a) The assembled MAS rotor. (b) Cross section view of the various internal components of the MAS rotor. The labeled parts in (a) and (b) are the zirconium rotor sleeve "1", spin tip "2", sample cell space "3", glass wool spacers "4" & "5", and end plugs "6" & "7". (c) The module for sample spinning inside the CF-MAS probe with the MAS rotor inserted in place. Labeled parts in (c) are the static injection tube "8" mounted in support/block "9", vacuum tube "10" mounted in support/block "11", pencil type driving mechanism for sample spinning "12", NMR RF coil "13", channel for variable temperature gas input "14", and magic angle adjustment "15".

circle to facilitate the injection of the reactants into the catalyst bed inside the sample cell "3". The end plug "7" contains similar holes to those of plug "6" but without a through center hole. The reason for this is that at a sample spinning rate of about 3 kHz, a "V" shape center hole inside the catalyst will be developed due to the centrifugal effect arising from sample spinning. The presence of a through center hole inside the end plug "7" will likely result in the channeling of reactants through this center hole.

Fig. 1c highlights the operation principles of our CF-MAS probe with the special MAS rotor (Fig. 1a) placed inside the spinning module of the probe. The injection tube "8" and carrier gas inlet are mounted into support block part "9" while the evacuation tube "10" and the outlet to the evacuation pump are mounted into block "11". A clearance of about 0.05 mm between the injection/evacuation tubes and the guiding holes inside the MAS rotor was made to prevent the direct contact of the static tubes and the spinning rotor. Therefore, like the design of Hunger and coworkers, our CF-MAS probe is an open system (*i.e.*, tubes are not sealed into the catalyst reactor) where an inlet gas flow pressure of 1.0 atmospheric pressure (101 kPa) is assumed.

## 3. Experimental

### 3.1. Catalysts

A tungsten heteropoly acid (HPA) with Keggin structure,  $\text{H}_3\text{PW}_{12}\text{O}_{40}\cdot n\text{H}_2\text{O}$ , supported on mesoporous silicalite (mesosilicalite), was used as the catalyst. The detailed synthesis of this material has been reported previously.<sup>25</sup> The properties of this catalyst have also been characterized using a combination of

XRD, TEM/SEM and  $^{31}\text{P}$  MAS NMR spectroscopy.<sup>25</sup> The parent meso-silicalite-1 has a BET surface area of  $418\text{ m}^2/\text{g}$  while the 28% weight percentage HPA/meso-silicalite-1 has a BET surface area of  $285\text{ m}^2/\text{g}$ .

### 3.2. NMR measurements

The *in situ* CF-MAS  $^1\text{H}$  and  $^{13}\text{C}$  experiments were performed on a Varian 500 MHz (11.7 T) NMR spectrometer with  $^1\text{H}$  and  $^{13}\text{C}$  Larmor frequencies of 500.19 and 125.79 MHz, respectively. A single pulse sequence with proton decoupling was used for  $^{13}\text{C}$  observation, where a recycle delay of 5 s, a 90 degree pulse angle using a pulse width of  $8\ \mu\text{s}$  and a decoupling field strength of approximately 25 kHz were employed. For  $^1\text{H}$  observation, a 30 degree angle pulse using a pulse width of  $4\ \mu\text{s}$  was used. A sample spinning rate of 3.5 kHz was used for all the measurement unless otherwise specified. Fine powders of meso-silicalite-1 and 28% HPA/meso-silicalite-1, with particle sizes of approximately  $5\ \mu\text{m}$ , were used. Meso-silicalite-1 or 28% HPA/meso-silicalite-1 powders of approximately 8 mm thickness were packed tightly inside the sample cell space of the CF-MAS rotor that was sandwiched between two layers of glass wool and the special end plugs as detailed in Fig. 1b. Sample temperature was calibrated using  $^{207}\text{Pb}$  MAS NMR on solid  $\text{Pb}(\text{NO}_3)_2$  powders at a sample spinning rate of 3.5 kHz according to procedures reported previously.<sup>26</sup> To ensure the accuracy of the temperature in the CF-MAS experiments, the sample spinning rate, the flow rate of the heating  $\text{N}_2$  gas, the driving and bearing nitrogen gas pressures were all kept the same as those for the calibrating  $^{207}\text{Pb}$  MAS NMR experiment.

## 4. Results

### 4.1. Sensitivity and temperature test

Using adamantane as a calibration test sample, the sensitivity of the 9.5 mm (ID of 8.0 mm) large-sample-CF-MAS probe was found to be approximately 2 times that of a standard

commercial 7.5 mm (ID of 6 mm) CP/MAS probe using a tightly packed sample cylinder of approximately 10 mm in height for both cases. This sensitivity enhancement is consistent with the expected volume increase, suggesting that the sensitivity of the 9.5 mm CF-MAS probe meets the expectations.

Using a home-made heating stack, under the conditions of  $\text{N}_2$  gas flow of 70 L/min for heating (separated from driving and bearing), a driving  $\text{N}_2$  gas pressure of 218.8 kPa (32.5 psi) and bearing  $\text{N}_2$  gas pressure of 251 kPa (37.3 psi), a stable sample spinning rate of 3.5 kHz was reached and a temperature up to 503 K (230 °C) was achieved based on the chemical shift value of the peak center (the highest peak position) of a  $^{207}\text{Pb}$  MAS NMR spectrum acquired on solid  $\text{Pb}(\text{NO}_3)_2$  powders. For the temperature calibration experiment, the dimensions of the solid  $\text{Pb}(\text{NO}_3)_2$  powder sample cylinder were 1.0 cm in height and 8 mm in OD. The  $^{207}\text{Pb}$  MAS NMR peak at 503 K covers a chemical shift range of about 19.6 ppm, corresponding to a temperature range from 489 to 517 K within the sample volume.

### 4.2. Validating the existence of flow

Gas flowing through a tube containing porous catalysts is facilitated by a pressure difference between the two ends of catalyst bed. However, the flow rate and flow pattern inside the catalyst bed depend on many factors including the pressure difference between both ends of the catalyst bed, the thickness and diameter of the bed, packing density of catalyst bed which is affected by sizes and geometries of the catalyst particles, the properties of the gases and the operating temperature. The following two sets of experiments were carried out to validate the existence of flow inside the catalyst bed; *i.e.*, with and without operation of the vacuum pump (a Diaphragm Membran-Vakuum Pumpe with a maximum  $1.7/2.0\text{ m}^3/\text{h}$  capacity from BrandTech Scientific, INC.). Since Meso-silicalite-1 is inert to 2-butanol at 346 K (see the *in situ*  $^{13}\text{C}$  CF-MAS results given in Fig. 5 below), *in situ* CF-MAS  $^1\text{H}$  NMR experiments with

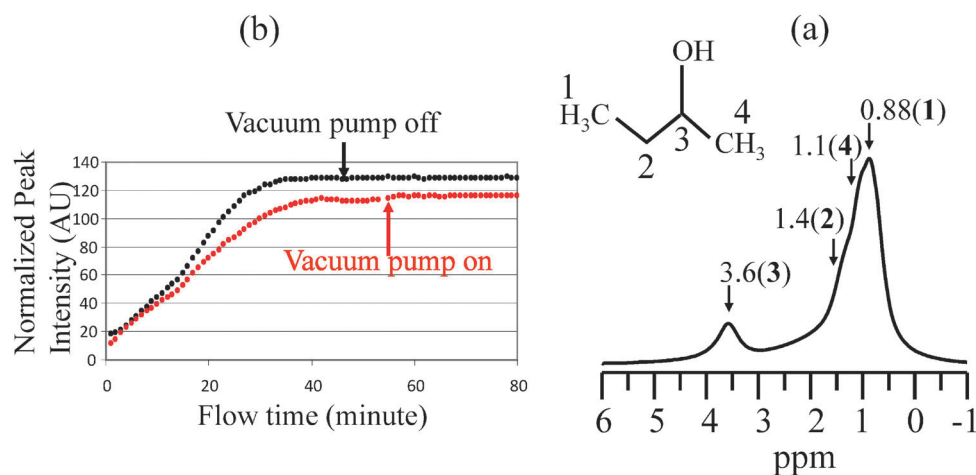


**Fig. 2** (a)  $^1\text{H}$  CF-MAS spectrum of 2-butanol after flowing an inert meso-silicalite-1 material for 40 min. The peak assignments are based on prior literature.<sup>37</sup> The integration range for obtaining the integrated spectral intensities shown in (b) from this and other spectra was from  $-1$  to 5 ppm. (b) The integrated spectral intensity of *in situ*  $^1\text{H}$  CF-MAS NMR spectra of 2-butanol flowing through meso-silicalite-1 as a function of time-on-stream with (red data) and without (black data) operation of the vacuum pump. These experiments were carried out at 346 K (73 °C) with a flow rate of 1.5 ml/h for 2-butanol in 100 SCCM of a  $\text{N}_2$  carrier gas, and at a sample spinning rate of 3.5 kHz. The spectrum corresponding to each data point was acquired using 32 scans with a recycle delay time of 2 s.

and without the vacuum pump turned on were carried out on this catalyst as a function of time by flowing 2-butanol at a rate of 1.5 ml liquid per hour. 2-butanol was injected/mixed into the flow of the carrier gas (dry N<sub>2</sub>) at room temperature (RT) using a combination of a syringe pump and mass flow controller outside the NMR magnet before flowing into the sample cell space of the probe. The flow rate of the carrier gas was set at 100 SCCM (standard cubic centimeters per minute). The results are summarized in Fig. 2.

Fig. 2a presents a typical CF-MAS <sup>1</sup>H NMR spectrum obtained after reaching steady flow conditions for 2-butanol in a N<sub>2</sub> flow. Fig. 2b plots the total integrated intensity of these spectra as a function of time after introducing the gas flow to the large-sample-CF-MAS probe reactor, demonstrating that the integrated <sup>1</sup>H peak intensity at 'steady' for the case when the vacuum pump is on is lower than that when the vacuum is off. This can only be possible if a significant portion of the gas flow passed through the catalyst bed. This is explained as follows based on consideration of the ideal gas law,  $P = (n/V) \times R \times T$ , where  $P$  is the pressure in pascal (Pa),  $R$  is the universal gas constant,  $T$  is the temperature in K, and  $(n/V)$  is the number of mole of gas molecules per unit volume. When the vacuum pump was off,  $P$  was approximately the same everywhere inside the catalyst bed at about 101 kPa (1 atm). However, when the vacuum pump was on,  $P$  linearly decreases from ~101 kPa at the injection end of the catalyst bed to quite low values at the other end where the vacuum pump was attached, resulting in a linear pressure drop inside the catalyst bed. Since  $T$  was almost constant in this reactor, a linear decrease in the value of  $(n/V)$  also resulted across the catalyst bed. Therefore, the total number of 2-butanol molecules in the reactor decreased, resulting in a corresponding decrease in the CF-MAS <sup>1</sup>H NMR integrated peak area at the new 'steady' state when the vacuum pump was on. One would, in fact, expect that the integrated peak intensity would have decreased to  $\frac{1}{2}$  that when the vacuum pump is off. The fact that the integrated intensity only decreased by about 15%, indicates that a major portion of the 2-butanol was inside the internal pores of the meso-silicalite-1, likely due to the capillary condensation. 2-butanol molecules located at the inter space between the catalyst particles are mostly affected by the flow. We note that efforts to obtain an improved flow that more accurately reflects typical steady-state catalytic reaction conditions in the *in situ* CF-MAS NMR probe are ongoing in our lab. Still, we believe that studies with the current probe can provide considerable useful data for studying catalytic reactions as highlighted in the following examples.

#### 4.3. Examples of Applications of the CF-MAS NMR probe

**4.3.1. *In situ* study of surface functional groups.** Fig. 3 demonstrates the use of the CF-MAS probe with an *in situ* <sup>1</sup>H CF-MAS NMR (at a sample spinning rate of 3.6 kHz) study of the effects of dehydration under various conditions on a 28 wt% HPA/meso-silicalite-1 catalyst. For a freshly prepared 28 wt% HPA/meso-silicalite-1 catalyst, two major peaks at about 1.0 (sharp) and 5.4 ppm (broad) and two shoulder peaks at about 1.65 and 3.6 ppm are observed (Fig. 3a). Since this freshly synthesized catalyst was exposed to air for about 24 h before acquiring Fig. 3a, it is expected that the catalyst surface was initially covered with

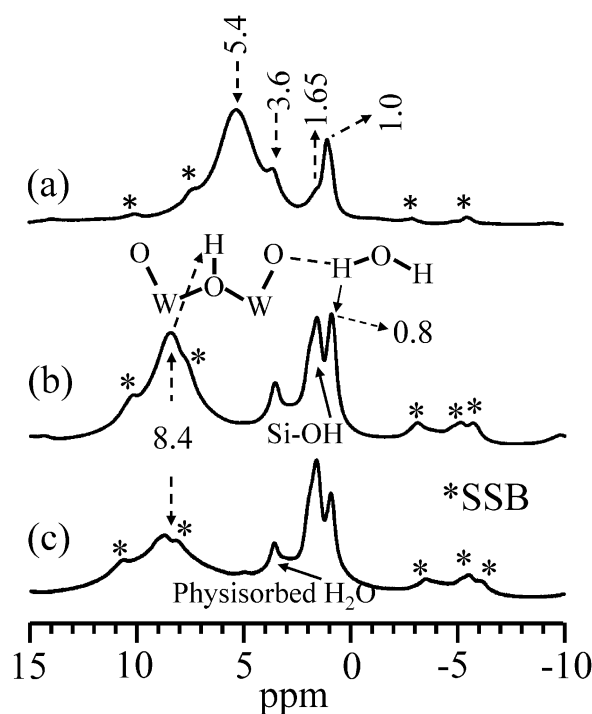


**Fig. 3** *In situ* <sup>1</sup>H MAS spectra acquired at a sample spinning rate of 3.6 kHz using the large-sample volume CF-MAS probe. (a) RT spectrum of freshly synthesized 28% HPA/meso-silicalite-1 acquired immediately after loading the sample into the probe and before flowing the carrier N<sub>2</sub> gas at 100 SCCM. (b) Spectrum acquired after *in situ* drying of the sample in (a) for 24 h at 373 K (100 °C) in a flow of 100 SCCM dry N<sub>2</sub> gas. (c) Acquired after (b) and after further flowing H<sub>2</sub>O at 1.5 ml/h in 100 SCCM N<sub>2</sub> carrier gas for 2 days, and then dried again at 393 K (120 °C) for 24 h after removal of H<sub>2</sub>O from the flow. Peaks denoted by "\*" are sample spinning sidebands. Each spectrum was acquired using 32 scans with a recycle delay time of 2 s.

significant quantities of weakly absorbed H<sub>2</sub>O molecules, even perhaps a thin layer of H<sub>2</sub>O, in addition to the various surface functional groups. Bulk H<sub>2</sub>O seems an unlikely candidate for the 5.4 ppm since its <sup>1</sup>H NMR peak should appear at about 4.8 ppm. While the 1.65 and 3.6 ppm peaks can be assigned to Si-OH and adsorbed H<sub>2</sub>O, respectively, based on a prior literature report,<sup>27</sup> the origin of the 1.0 ppm is more difficult to assign.

After *in situ* drying of the 28 wt% HPA/meso-silicalite-1 catalyst; *i.e.*, removal of weakly absorbed surface H<sub>2</sub>O molecules by constantly flowing dry nitrogen gas at 100 °C for 24 h, the *in situ* <sup>1</sup>H MAS spectrum, given in Fig. 3b, shows some interesting changes. First, a broad peak at about 8.4 ppm that was not observed in the fresh catalyst appears as the major peak, in a position that typically corresponds to highly acidic protons. It has been proposed that, for supported HPA on porous silicate materials,<sup>28</sup> the acidic protons (Brønsted acid sites) are the bridging W-OH-W groups associated with HPA. Thus, it seems reasonable to assign the 8.4 ppm peak to the tungsten bridging hydroxyl (W-OH-W) protons. This assignment is consistent with prior <sup>1</sup>H MAS NMR studies of H<sub>3</sub>PW<sub>12</sub>O<sub>40</sub> (HPA) and HPA supported on porous SiO<sub>2</sub> materials using a sealed MAS rotor.<sup>29–32</sup> Also of note is that the three peaks with chemical shifts less than ~4 ppm are now well resolved. The peak centers for the 3.6 and 1.65 ppm

remain unchanged. However, the peak originally at about 1.0 ppm is shifted to about 0.8 ppm. The 0.8 ppm peak has been assigned to the proton in the H<sub>2</sub>O molecule that is hydrogen bonded to the oxygen in WO group.<sup>27</sup> Thus, by removing weakly bound surface H<sub>2</sub>O molecules at moderate temperature using *in situ* drying, surface proton functional groups can be studied effectively using CF-MAS <sup>1</sup>H NMR.

Fig. 3c further highlights the usefulness of studying the stability of the catalyst by *in situ* CF-MAS <sup>1</sup>H NMR. In this example, water was flowing at a rate of 1.5 ml/h and at 100 °C for 48 h, followed by *in situ* drying for 24 h prior to acquiring an *in situ* CF-MAS <sup>1</sup>H NMR spectrum. The spectral resolution in this spectrum (Fig. 3c) is similar to that of Fig. 3b except the relative peak intensity corresponding to the Si-OH groups at 1.65 ppm is noticeably enhanced. This is clear evidence that some of the meso-silicalite-1 surface, originally covered by HPA, is now exposed. This result suggests some agglomeration of the HPA particles over time due to the constantly flowing H<sub>2</sub>O through the catalyst bed. This interesting observation is perhaps consistent with the hypothesis that the role of water is to recover the Keggin structure. However, during such a process H<sub>2</sub>O apparently reduces the degree of HPA dispersion on the support surface, a somewhat undesirable side effect.

**4.3.2. *In situ* study of reaction dynamics using <sup>1</sup>H CF-MAS NMR.** Due to its large gyromagnetic ratio and its essentially 100% of natural abundance, <sup>1</sup>H MAS NMR offers the highest NMR sensitivity and is attractive for *in situ* investigations of catalytic reaction dynamics. Using the large-sample-volume CF-MAS probe, an *in situ* <sup>1</sup>H MAS NMR spectrum with excellent S/N ratios can be acquired in a single scan and, thus, with a time resolution as short as one second. However, more scans can often be used if the reaction is not too rapid, such as was the case for the 2-butanol dehydration reaction studied here.

Fig. 4 shows a series of spectra selected from *in situ* <sup>1</sup>H CF-MAS NMR studies of 2-butanol dehydration over 28% HPA/meso-silicalite-1 as a function of the flow time, where a liquid flow rate of 1.5 ml/h for 2-butanol carried by 100 SCCM of dry N<sub>2</sub> gas at RT was used. The reaction temperature inside the sample cell was held at 73 °C. Before the 2-butanol stream reached the catalyst bed (set as time zero), the *in situ* CF-MAS <sup>1</sup>H NMR spectrum is the same as that of Fig. 3c due to the fact that the data in Fig. 4 were acquired immediately after those in Fig. 3c. A distinct reaction product peak, located at about 5.4 ppm, is clearly observed in the spectrum at a time-on-stream of about 8 min. This peak is assigned to both the *cis* and *trans* CH protons in the 2-butene molecule based on a prior literature report.<sup>33</sup> The intensity of the 5.4 ppm peak increases with flow time, and a plateau is reached at a flow time of approximately 30 min. The peak corresponding to the CH proton in 2-butanol, labeled as the “3” position, is found at about 3.6 ppm and overlaps with the peak of adsorbed H<sub>2</sub>O. The 3.6 ppm peak also increases with the flow time but reached a plateau at an earlier flow time of approximately 18 min. Other peaks related to the products and the reactants overlap over a chemical shift range from 0 to about 2.2 ppm as indicated in Fig. 4. The data presented in Fig. 4 clearly demonstrates that under the condition of constantly flowing reactant over the catalyst bed, a steady-state condition is established where the products are eluted out of

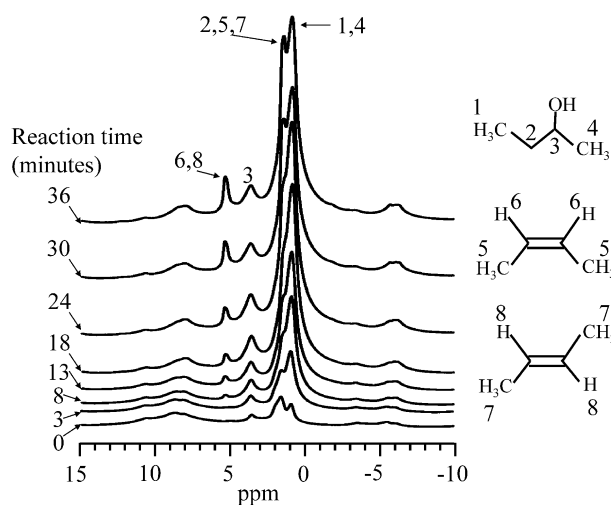


**Fig. 4** Stack plot of selected spectra from *in situ* <sup>1</sup>H CF-MAS NMR experiments of 2-butanol catalysis over 28% HPA/meso-silicalite-1 as a function of the flow time. The flow rates were 1.5 ml/h for 2-butanol and 100 SCCM for the N<sub>2</sub> carrier gas, respectively. Each spectrum was acquired using 32 scans and a recycle delay time of 2 s. The sample spinning rate was 3.5 kHz for all the measurements.

the catalyst bed and subsequently carried away by the carrier gas are equal to the products generated over the same time period. This offers a stable condition for investigating questions such as how the reactants are interacting with the catalyst surfaces as a function of reaction conditions (*e.g.*, temperature), including the identification of possible stable reaction intermediates/transition states.

Although <sup>1</sup>H MAS NMR is highly sensitive, the spectral resolution is limited. As a result, in this example the two isomers of the reaction product of 2-butanol dehydration, *cis*- and *trans*-2-butene, cannot be differentiated. This limitation can be partially overcome by *in situ* <sup>13</sup>C CF-MAS NMR due to its much higher spectral resolution and larger chemical shift range, hence a much higher sensitivity to the subtle structural changes.

**4.3.3. Natural abundance <sup>13</sup>C CF-MAS NMR.** Fig. 5a shows an *in situ* natural abundance <sup>13</sup>C CF-MAS NMR spectrum of 2-butanol flowing through meso-silicalite-1 at a flow rate of 1.5 ml/h and at a reaction temperature of 73 °C. Only four peaks (9.9, 23.3, 32.6 and 70.6 ppm), corresponding to the four carbons associated with 2-butanol, are observed, demonstrating that meso-silicalite-1 is inert (*i.e.*, not reactive) to 2-butanol. In contrast, when 2-butanol is flowing through a 28% HPA/meso-silicalite-1 catalyst bed under the same experimental conditions, peaks corresponding to the reaction products are observed at 11.8 ppm for the methyl carbon of *cis*-2-butene, 16.9 ppm for the methyl carbon of *trans*-2-butene, and 126.3 ppm for the CH carbons in both the *cis*-, and *trans*-2-butene. The peak area ratio of the *trans*- to *cis*-2-butene is found to be about 2.5 to 1.

The above peak assignments are based on results tabulated in computer databases, *i.e.*, ACD/NMR Databases by ACD/Labs (<http://www.acdlabs.com>) on the <sup>13</sup>C isotropic chemical shift values for 2-butanol, *cis*-2-butene, *trans*-2-butene, 1-butene, propene and 2-methylpropene (see the results summarized in Fig. 5). The latter four molecules have been reported as the only reaction products of the 2-butanol dehydration reaction



in 2-butanol, likely *via* hydrogen bonding with tungsten bridging acidic proton and oxygens double bonded to tungsten, respectively. Residual adsorbed reaction intermediates, coke products, and other 'spectator' species that may be precursors to coke can also be detected at natural  $^{13}\text{C}$  abundance after reaction. Such a spectrum obtained after 2-butanol dehydration over a 28% HPA/meso-silicalite-1 catalyst was found to consist of NMR peaks associated with aliphatic carbon networks that lack either direct C–O or C=C bonds. Furthermore, we show that the surface functional groups of HPA/meso-silicalite-1 can be identified under the condition of *in situ* drying using  $^1\text{H}$  CF-MAS NMR, where the Brønsted acid sites of the supported HPA are found at about 8.4 ppm after removing weakly absorbed  $\text{H}_2\text{O}$ . We have also demonstrated that the reaction dynamics of 2-butanol dehydration using HPA/meso-silicalite-1 as catalyst can be explored using  $^1\text{H}$  CF-MAS NMR.

## Acknowledgements

This research was supported by the U. S. Department of Energy (DOE), Office of Basic Energy Sciences, Division of Chemical Sciences, Biosciences and Geosciences. All experiments were performed in the Environmental Molecular Sciences Laboratory, a national scientific user facility sponsored by the DOE's Office of Biological and Environmental Research, and located at Pacific Northwest National Laboratory (PNNL). PNNL is a multi-program national laboratory operated for the DOE by Battelle Memorial Institute under Contract DE-AC06-76RLO 1830. Prof. Enrique Iglesia is acknowledged for his valuable suggestions about improving the flow through the catalyst bed, and Ms. Mary Hu is acknowledged for her help with the preparation of the figures.

## References

- 1 *NMR Techniques in Catalysis*, ed. A. T. a. P. A. Bell, Marcel Dekker, Inc., 1994.
- 2 M. W. Anderson, J. Dwyer, G. J. Hutchings, D. F. Lee, M. Makarova and B. Zibrowius, *Catal. Lett.*, 1995, **31**, 377.
- 3 A. Buchholz, W. Wang, M. Xu, A. Arnold and M. Hunger, *J. Phys. Chem. B*, 2004, **108**, 3107.
- 4 E. G. Derouane, H. Y. He, S. B. Derouane-Abd Hamid and I. I. Ivanova, *Catal. Lett.*, 1999, **58**, 1.
- 5 M. Hunger, *Prog. Nucl. Magn. Reson. Spectrosc.*, 2008, **53**, 105.
- 6 M. Hunger and T. Horvath, *J. Chem. Soc., Chem. Commun.*, 1995, 1423.
- 7 M. Hunger and T. Horvath, *J. Catal.*, 1997, **167**, 187.
- 8 M. Hunger, T. Horvath and J. Weitkamp, *Stud. Surf. Sci. Catal.*, 1997, **105**, 853.
- 9 M. Hunger, U. Schenk, M. Seiler and J. Weitkamp, *J. Mol. Catal. A: Chem.*, 2000, **156**, 153.
- 10 M. Hunger, M. Seiler and T. Horvath, *Catal. Lett.*, 1999, **57**, 199.
- 11 I. I. Ivanova and Y. G. Kolyagin, *Chem. Soc. Rev.*, 2010, **39**, 5018.
- 12 T. R. Krawietz, D. K. Murray and J. F. Haw, *J. Phys. Chem. A*, 1998, **102**, 8779.
- 13 M. Seiler, U. Schenk and M. Hunger, *Catal. Lett.*, 1999, **62**, 139.
- 14 I. I. Ivanova, *Colloids Surf., A*, 1999, **158**, 189.
- 15 J. F. Haw, *Abstr. Pap. Am. Chem. S.*, 1998, **215**, U467.
- 16 J. F. Haw, *Abstr. Pap. Am. Chem. S.*, 1998, **215**, U482.
- 17 J. F. Haw, *Abstr. Pap. Am. Chem. S.*, 1999, **218**, U668.
- 18 J. F. Haw, *Top. Catal.*, 1999, **8**, 81.
- 19 J. F. Haw, P. W. Goguen, T. Xu, T. W. Skloss, W. G. Song and Z. K. Wang, *Angew. Chem., Int. Ed.*, 1998, **37**, 948.
- 20 J. F. Haw and T. Xu, *Adv. Catal.*, 1998, **42**, 115.
- 21 T. A. Carpenter, J. Klinowski, D. T. B. Tennakoon, C. J. Smith and D. C. Edwards, *J. Magn. Reson.*, 1986, **68**, 561.
- 22 T. Xu and J. F. Haw, *Top. Catal.*, 1997, **4**, 109.
- 23 W. P. Zhang, X. H. Bao, X. W. Guo and X. S. Wang, *Catal. Lett.*, 1999, **60**, 89.
- 24 D. I. Hoult and R. E. Richards, *J. Magn. Reson.*, 1976, **24**, 71.
- 25 J. Liu, K. K. Zhu, J. Z. Hu, X. Y. She, Z. M. Nie, Y. Wang, C. H. F. Peden and J. H. Kwak, *J. Am. Chem. Soc.*, 2009, **131**, 9715.
- 26 L. C. M. van Gorkom, J. M. Hook, M. B. Logan, J. V. Hanna and R. E. Wasylishen, *Magn. Reson. Chem.*, 1995, **33**, 791.
- 27 J. E. Herrera, J. H. Kwak, J. Z. Hu, Y. Wang, C. H. F. Peden, J. Macht and E. Iglesia, *J. Catal.*, 2006, **239**, 200.
- 28 E. Iglesia, J. Macht, M. J. Janik and M. Neurock, *J. Am. Chem. Soc.*, 2008, **130**, 10369.
- 29 A. Thomas, C. Dablemont, J. M. Basset and F. Lefebvre, *C. R. Chim.*, 2005, **8**, 1969.
- 30 V. M. Mastikhin, S. M. Kulikov, A. V. Nosov, I. V. Kozhevnikov, I. L. Mudrakovsky and M. N. Timofeeva, *J. Mol. Catal.*, 1990, **60**, 65.
- 31 M. Misono, S. Uchida and K. Inumaru, *J. Phys. Chem. B*, 2000, **104**, 8108.
- 32 J. P. Amoureux, S. Ganapathy, M. Fournier, J. F. Paul, L. Delevoye and M. Guelton, *J. Am. Chem. Soc.*, 2002, **124**, 7821.
- 33 R. K. Harris and B. R. Howes, *J. Mol. Spectrosc.*, 1968, **28**, 191.
- 34 J. F. Haw, B. R. Richardson, I. S. Oshiro, N. D. Lazo and J. A. Speed, *J. Am. Chem. Soc.*, 1989, **111**, 2052.
- 35 A. Philippou, J. Dwyer, A. Ghanbari-Siahkali, C. Paze and M. W. Anderson, *J. Mol. Catal. A: Chem.*, 2001, **174**, 223.
- 36 A. G. Stepanov, M. V. Luzgin, V. N. Romannikov, V. N. Sidelnikov and E. A. Paukshtis, *J. Catal.*, 1998, **178**, 466.
- 37 L. M. Jackman and N. S. Bowman, *J. Am. Chem. Soc.*, 1966, **88**, 5565.